Inorganica Chimica Acta 446 (2016) 6–12

Contents lists available at ScienceDirect

Inorganica Chimica Acta

journal homepage: www.elsevier.com/locate/ica

# Structural analysis and IR-spectroscopy of a new anilinium hydrogenselenite hybrid compound: A subtle structural phase transition

Radhwane Takouachet [a], Rim Benali-Cherif [a], El-Eulmi Bendeif [b,c,*], Nourredine Benali-Cherif [a,d], Sébastien Pillet [b,c], Dominik Schaniel [b,c]

[a] Laboratoire des Structures, Propriétés et Interactions InterAtomiques, Université Abbes Laghrour-Khenchela, 40000 Khenchela, Algeria
[b] Université de Lorraine, CRM2, UMR 7036, Vandoeuvre-les-Nancy F-54506, France
[c] CNRS, CRM2, UMR 7036, Vandoeuvre-les-Nancy F-54506, France
[d] Ecole Nationale Polytechnique-Constantine (ENPC), 25000 Constantine, Algeria

ARTICLE INFO

*Article history:*
Received 12 October 2015
Received in revised form 19 February 2016
Accepted 22 February 2016
Available online 2 March 2016

*Keywords:*
Phase transition
X-ray diffraction
IR spectroscopy
Molecular disorder
Hybrid compound

ABSTRACT

An interesting structural behavior has been detected and characterized in a new anilinium based compound by single crystal X-ray diffraction measurements and infrared spectroscopy. The temperature dependent structural investigation reveals that the studied compound undergoes a subtle non-centrosymmetric to centrosymmetric structural phase transition. At room temperature the crystal structure is non-centrosymmetric and is characterized by an important disorder in the organic part where the independent aromatic rings are rotated around the C1—C4 and C7—C10 molecular axis by 52.06(6)° and 56.25 (4)° respectively. By decreasing the temperature to 100 K the organic cation is less disordered and the rotation angle of the aromatic rings changes to 54.73(2)°. As a consequence, the low temperature structure becomes centrosymmetric. The infrared spectra recorded on cooling and heating the sample in the temperature range of 300–9 K support this analysis. The ammonium group ($NH_3$) is significantly affected by the temperature change. This effect results, when cooling the sample below 140 K, in the appearance of a new vibrational band corresponding to the ($NH_3$)-wagging modes at 705 $cm^{-1}$. The phenomenon is completely reversible and the new vibrational band disappears upon heating the sample above 140 K. Moreover, the $\nu$(C–N)-stretching and the ($NH_3$)-scissoring modes are also affected by the temperature variation as can be seen in the spectral ranges of 1250–1400 $cm^{-1}$ and 1610–1635 $cm^{-1}$ respectively. The spectroscopic results are complementary to the structural analysis and indicate that the structural phase transition is correlated with the molecular rotation of the aromatic moieties around the C1—C4 axis that affect the different vibrational modes of the ammonium group.



## 1. Introduction

The organic–inorganic hybrid compounds have been extensively studied over the last few decades for their specific properties and potential applications. These compounds display a wide range of molecular interactions network, from strong ionic and hydrogen bonding to weak van der Waals contacts. It is well established that hydrogen bonding play a key role in molecular association processes and therefore it provides a source of novel materials with very promising physical, chemical and biological properties [1–13]. The organic–inorganic salts based on amino acids, amines and their derivatives are among the most investigated systems owing to their use in drug design processing and in non-linear optical devices. For instance, aniline derivatives are used as starting materials in several industrial and pharmaceutical processes because they can serve as precursors in the synthesis of dyes, pesticides and antioxidants [14,15]. They are also used in the elaboration of electro-optical materials with non-linear optical responses [16]. In this respect, a number of ortho- and para-substituted anilinium derivatives exhibit very interesting optical properties associated with structural phase transitions [17,18]. It has been shown that 2-methoxyanilinium nitrate [19], p-nitroanilium nitrate [20], p-nitroanilium perchlorate [21] have very promising third order nonlinear optical properties. Very recently, the crystal structure and the optical properties of p-nitroanilium sulfate have been described by Bouchouit and co-workers [22]. It was found that second order optical properties are correlated to the reversible structural phase transition that occurs at 338 K. Some of inorganic

* Corresponding author at: Université de Lorraine, CRM2, UMR 7036, Vandoeuvre-les-Nancy F-54506, France. Tel.: +33 (0)3 83 68 48 70; fax: +33 (0)3 83 68 43 00.
*E-mail address:* el-eulmi.bendeif@univ-lorraine.fr (E.-E. Bendeif).

http://dx.doi.org/10.1016/j.ica.2016.02.047
0020-1693/

anilinium and substituted anilinium salts exhibit structural phase transitions induced by order/disorder of the ammonium ($NH_3^+$) groups [23]. The spectroscopic studies of anilinium halides [24] showed a subtle phase transition associated with unexpected structural features. The present work, continues a series of our research since several years on hybrid compounds of anilinium derivative salts [25–30]. It is noteworthy that the structural analysis of hybrid compounds based on selenious acid and amine is still scarce and quite disparate. So far, only nine crystal structures of amine–selenious compounds are deposited in the *Cambridge Structural Database* (CSD, Version 1.17, 2015) [31].

Herein, we report the X-ray single crystal structural analysis of a new anilinium–selenious hybrid compound. The temperature dependent structural investigation reveals that the studied compound undergoes a subtle non-centrosymmetric to centrosymmetric structural phase transition. In order to get more insight on this interesting and subtle behavior, we discuss in this paper the relevant structural parameters we obtained from variable temperature single crystal measurements, infrared spectroscopy and DSC analysis.

## 2. Experimental

### 2.1. Synthesis and crystallization

Crystals of anilinium hydrogenselenite monohydrate: $[(C_6H_8N)^+, (HSeO_3)^-, H_2O]$ were obtained from an aqueous solution of selenious acid added to aniline in the stoichiometric ratio 1:1 at room temperature. After four weeks of slow evaporation, small colorless single crystals appeared.

### 2.2. Single crystal X-ray diffraction and structure refinement details

The temperature dependent single crystal X-ray diffraction experiments were performed on a SuperNova Dual Wavelength Microfocus diffractometer equipped with a 135 mm Atlas CCD detector, using Mo Kα radiation ($\lambda$ = 0.71073 Å). All the measurements were carried out on the same single crystal. The temperature of the sample was controlled with a liquid-nitrogen Oxford Cryostream cooling device. Three different data sets have been collected at 293 K, 225 K and 100 K respectively. In order to ensure high redundancies, the intensity data were accurately collected using $\omega$ oscillation scans of 1° per frame repeated at different φ positions. The exposure time was 30 s per frame for the 100 K data and 60 s for the 225 K and 293 K data. Coverage of reciprocal space was more than 99.9% complete to ($\sin\theta_{max}/\lambda$) of 0.765 $Å^{-1}$. The unit cell determination and data integration were carried out using the *CrysAlis* program suite [32]. Absorption effects were corrected by numerical methods based on crystal face indexing. The structure was solved by direct methods and successive Fourier difference syntheses and refined against $F^2$ by weighted full-matrix least-squares methods using the SHELXL97 program [33]. All non-hydrogen atoms were refined anisotropically, hydrogen atoms were located in difference Fourier maps and treated using a riding model, constraining the isotropic displacement parameters to the appropriate values of the attached atoms (1.2 times for C atoms and 1.5 times for N and O atoms). One notes that the H atoms of water molecules and hydroxyl groups were refined with restrained O–H distances (O–H = 0.96(2) Å). These values are much more appropriate compared to the standard DFIX restraints (0.84(2) Å) used with SHELXL and lead to more realistic structural parameters as also shown by the calculated Fourier difference maps obtained after the refinement of the H atoms. The FLAT (for the flat geometry) and DELU (*for rigid group*) restraints were also used for the refinement of the disordered aromatic rings.

All calculations were carried out using the WinGX software package [34]. The crystallographic data, measurements and refinement details are summarized in Table 1.

### 2.3. Calorimetric measurements

The differential scanning calorimetry (DSC) experiments were performed on DSC1 Mettler-Toledo instrument equipped with a high sensitivity DSC HSS8 sensor. 2.18 mg of microcrystalline powder of anilinium hydrogenselenite monohydrate were first sealed in an aluminum pan and then submitted to two subsequent cooling–heating cycles in the 123–300 K temperature range. The measurements were made under nitrogen at atmospheric pressure and the cooling and heating scan rates were kept at 5 K $min^{-1}$.

### 2.4. Infrared spectroscopy

The infrared spectra were recorded in the spectral range of 400–4000 $cm^{-1}$, using a Nicolet 5700 FT-IR spectrometer with a resolution of 2 $cm^{-1}$. The sample was ground, mixed with KBr and pressed into pellets. The KBr pellets were glued with silver paste on a copper cold-finger of an Oxford closed-cycle cryostat, equipped with KBr windows. The measurements were performed by cooling and heating the KBr pellets in the temperature range of 300–9 K. The temperature was regulated by a MercuryiTC temperature controller in the range of 9–300 K and the vacuum inside the cryostat was $10^{-4}$ mbar.

## 3. Results and discussion

### 3.1. The crystal structure

The crystal structure of $[(C_6H_8N)^+, (HSeO_3)^-, H_2O]$ was first studied at room temperature. It belongs to the triclinic *P*1 space group. The asymmetric unit consists of two structurally independent and disordered anilinium organic cations $(C_6H_8N)^+$, two hydrogenselenite anions $(HSeO_3)^-$ and one water molecule as shown in Fig. 1. The selected structural parameters are given in Table 2.

The crystal packing is built of layers parallel to the *bc* plane of alternating anilinium cations and hydrogenselenite anions interconnected by N—H...O hydrogen bonds. The water molecules are located within the anionic layers and allow therefore the connection between the anionic groups by a pseudo-centrosymmetric O—H...O hydrogen bond. One notes that there are no hydrogen bonds between the organic cations (see Fig. 2).

The geometrical features of the inorganic anions $(HSeO_3)^-$ (Table 2) are typical and are in good agreement with those observed in similar compounds [35]. However the molecular structure shows an important disorder of the organic part where the two symmetry independent aromatic rings are rotated around the C1—C4 and C7—C10 molecular axes by 52.06(6)° and 56.25 (4)° respectively. In order to determine the nature of such atypical disorder (static or dynamic) we investigated the temperature dependent changes in the 100–293 K temperature range of: (i) the unit-cell parameters and (ii) the structural parameters.

### 3.2. Thermal behavior

#### 3.2.1. Temperature dependence of the unit cell parameters

The temperature dependent changes of selected unit cell parameters (*a*, *b* and *V*) in the 293–100 K temperature range are depicted in Fig. 3 (for more details see Table 1S in Supporting information). By cooling the sample from room temperature (293 K) to 100 K one can clearly distinguish two different behaviors: from

**Table 1**
Main crystallographic data and structure refinement details for $C_6H_{11}NO_4Se$ at 100, 225 and 293 K.

| | | | |
|---|---|---|---|
| *Crystal data* | | | |
| Empirical formula | $C_6H_{11}NO_4Se$ | $C_6H_{11}NO_4Se$ | $C_6H_{11}NO_4Se$ |
| Molecular weight (g/mol) | 240.12 | 240.12 | 240.12 |
| $T$ (K) | 100 | 225 | 293 |
| Calculated density (g/cm$^3$) | 1.758 | 1.734 | 1.726 |
| Crystal system | triclinic | triclinic | triclinic |
| Space group | $P\bar{1}$ | $P1$ | $P1$ |
| $a$ (Å) | 4.7212(2) | 4.7423(3) | 4.7635(4) |
| $b$ (Å) | 9.3681(3) | 9.4263(8) | 9.4658(9) |
| $c$ (Å) | 11.1290(3) | 11.1599(7) | 11.184(1) |
| $\alpha$ (°) | 107.297(3) | 107.271(6) | 107.238(8) |
| $\beta$ (°) | 92.294(3) | 92.652(6) | 92.815(8) |
| $\gamma$ (°) | 103.549(3) | 103.370(7) | 103.301(8) |
| $V$ (Å$^3$) | 453.68(3) | 459.91(6) | 464.97(8) |
| $Z$ | 2 | 2 | 2 |
| $\mu$ (mm$^{-1}$) | 4.12 | 4.06 | 4.01 |
| Crystal size (mm) | 0.40 × 0.30 × 0.20 | 0.40 × 0.30 × 0.20 | 0.40 × 0.30 × 0.20 |
| *Data collection* | | | |
| Diffractometer, radiation | SuperNova Dual Wavelength Microfocus diffractometer, Mo K$\alpha$ $\lambda$ = 0.71073 Å | | |
| $T_{minimum}$, $T_{maximum}$ | 0.334, 0.825 | 0.303, 0.798 | 0.301, 0.789 |
| No. of measured, independent and observed [$I > 2\sigma(I)$] reflections | 14837, 3183, 3035 | 14120, 5941, 4197 | 8107, 5308, 3211 |
| $R_{int}$ | 0.035 | 0.056 | 0.077 |
| (sin $\theta/\lambda)_{maximum}$ (Å$^{-1}$) | 0.764 | 0.765 | 0.767 |
| *Refinement* | | | |
| $R[F^2 > 2\sigma(F^2)]$, $wR(F^2)$, $S$ | 0.018, 0.043, 1.05 | 0.048, 0.099, 1.06 | 0.070, 0.258, 1.02 |
| No. of unique reflections | 3183 | 5941 | 5308 |
| No. of parameters | 194 | 316 | 316 |

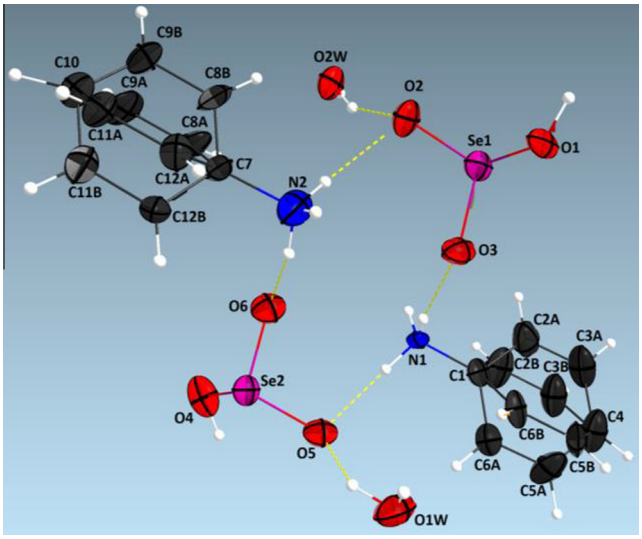


**Fig. 1.** The asymmetric unit of $[(C_6H_8N)^+, (HSeO_3)^-, H_2O]$, showing the atom-labeling scheme. The two symmetry independent aromatic rings are disordered over two orientations. Displacement ellipsoids are drawn at the 50% probability level and H atoms are shown as small gray spheres of arbitrary radii.

293 to 150 K, the cell parameters exhibit a similar behavior and show continuous structure contraction ($\Delta a/a \sim -1\%$, $\Delta b/b \sim -1.2\%$ and $\Delta V/V \sim -1.9\%$ referring to 293 K). However, at temperatures between 140 and 110 K we observe an anomalous behavior with discontinuity in cell parameters then decrease again at 100 K. To get more insight on this subtle and unexpected thermal behavior, we performed a calorimetric analysis in the temperature range of 123–300 K.

### 3.2.2. The DSC analysis

The thermal behavior of the title compound has also been studied using differential scanning calorimetry (DSC), in order to investigate an occurrence of phase transition that may explain the disorder of the organic cation. The DSC results are shown in Fig. 4. As can be seen, the DSC curves did not show any evident signature for a possible phase transition at temperatures between 300 K and 123 K. It is also noteworthy that the different DSC curves measured with different cooling–heating rates (5 K min$^{-1}$ and 10 K min$^{-1}$) did not show any significant effects that can be related to a possible structural phase transition.

**Table 2**
Selected structural parameters, bond lengths (Å) and bond angles (°) for $C_6H_{11}NO_4Se$ at 100, 225 and 293 K.

| | (100 K) | (225 K) | (293 K) |
|---|---|---|---|
| *Bond lengths (Å)* | | | |
| Se1—O3 | 1.6654(8) | 1.676(14) | 1.64(2) |
| Se1—O2 | 1.6789(9) | 1.682(14) | 1.71(2) |
| Se1—O1 | 1.7735(8) | 1.752(14) | 1.76(2) |
| Se2—O6 | – | 1.646(14) | 1.64(2) |
| Se2—O5 | – | 1.659(15) | 1.67(2) |
| Se2—O4 | – | 1.790(11) | 1.789(16) |
| N1—C1 | 1.4611(15) | 1.463(2) | 1.48(3) |
| N2—C7 | | 1.455(2) | 1.45(3) |
| *Bond angles (°)* | | | |
| O3—Se1—O2 | 104.05(4) | 103.7(7) | 103.7(11) |
| O3—Se1—O1 | 97.02(4) | 97.1(7) | 97.8(11) |
| O2—Se1—O1 | 100.94(4) | 101.2(7) | 101.1(10) |
| O6—Se2—O5 | | 104.8(7) | 105.2(11) |
| O6—Se2—O4 | | 97.0(6) | 101.6(10) |
| O5—Se2—O4 | | 96.6(9) | 100.6(7) |

### 3.2.3. Structures at low temperatures (225 K and 100 K)

The asymmetric units of the title compound at 225 K and 100 K are shown in Fig. 5. The crystal structure at 225 K remains triclinic, as at room temperature, with a non-centrosymmetric space group $P1$. When the temperature decreases to 100 K, the space group changed from $P1$ to $P\bar{1}$. To verify the structural phase transition, the low temperature (100 K) crystal structure has been resolved and refined in both $P1$ and $P\bar{1}$ space groups. The structural model was essentially the same, however the centrosymmetric ($P\bar{1}$) struc-

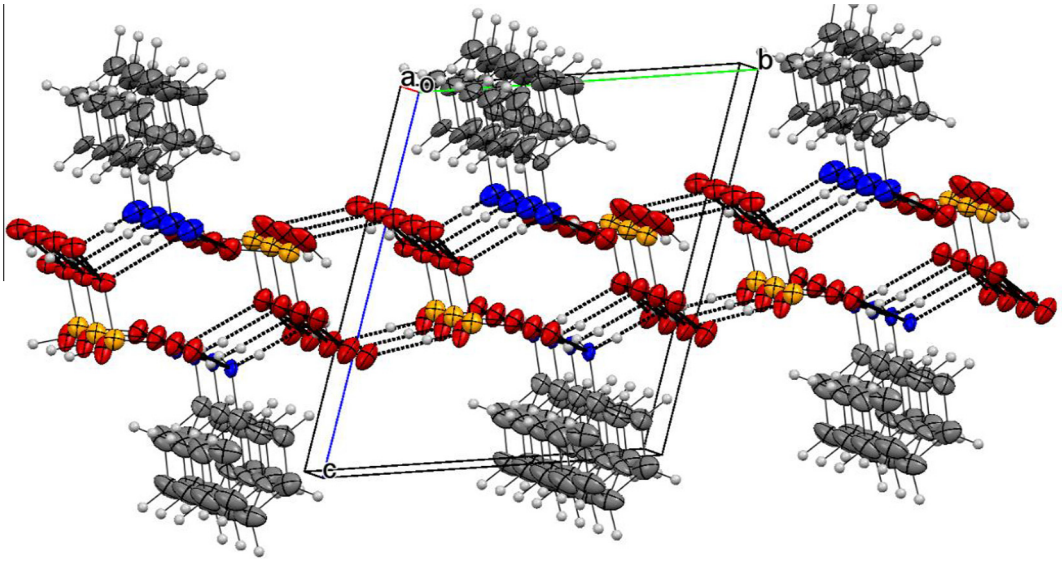


**Fig. 2.** The crystal packing of the title compound, showing the different bonding schemes of anilinium cations and the anionic part.

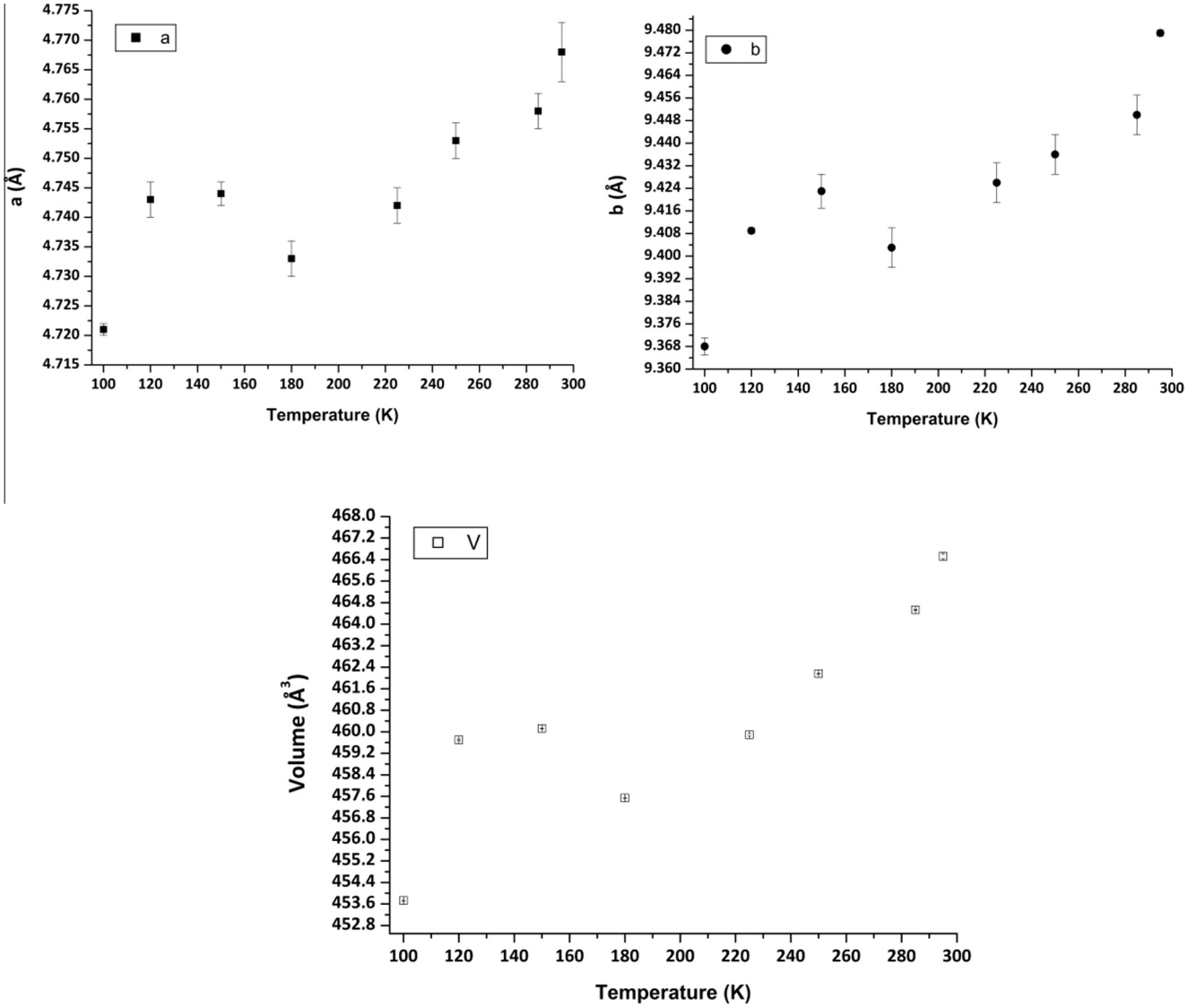


**Fig. 3.** Temperature dependence of the unit-cell parameters $a$ (Å), $b$ (Å) and $V$ (Å$^3$).

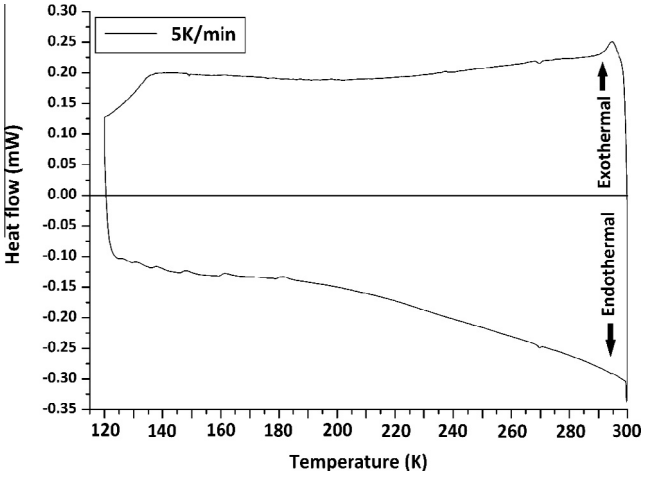


**Fig. 4.** Differential scanning calorimetry (DSC) curves of $[(C_6H_8N)^+, (HSeO_3)^-, H_2O]$ upon cooling and heating the crystalline sample in the 300–123 K temperature range.

**Table 3**
Selected hydrogen bonds parameters (Å, °).

| *D*—H···*A* | *D*—H (Å) | H···*A* (Å) | *D*···*A* (Å) | *D*—H···*A* (°) |
|---|---|---|---|---|
| *(100 K)* | | | | |
| N1—H1B···O3$^{i}$ | 0.923(18) | 1.869(18) | 2.7916(13) | 177.7(16) |
| N1—H1C···O2$^{ii}$ | 0.905(19) | 1.908(19) | 2.8131(13) | 178.1(17) |
| N1—H1A···O3 | 0.877(18) | 1.886(18) | 2.7536(13) | 169.7(17) |
| O1—H1···O1W | 0.9786(9) | 1.6688(9) | 2.6276(13) | 165.47(6) |
| O1W—H1W···O2$^{iii}$ | 0.977(2) | 1.799(5) | 2.7643(12) | 168.9(19) |
| O1W—H2W···O2$^{iv}$ | 0.976(2) | 1.818(4) | 2.7880(12) | 172(2) |
| *(225 K)* | | | | |
| N1—H1A···O5 | 0.90 | 1.94 | 2.83(2) | 172.6 |
| N1—H1B···O3$^{i}$ | 0.90 | 1.91 | 2.80(2) | 175.0 |
| N1—H1C···O3 | 0.90 | 1.88 | 2.75(2) | 163.4 |
| N2—H2A···O6$^{v}$ | 0.90 | 1.91 | 2.80(2) | 169.7 |
| N2—H2B···O2 | 0.90 | 1.93 | 2.82(2) | 169.6 |
| N2—H2C···O6 | 0.90 | 1.89 | 2.77(2) | 168.6 |
| O1W—H1W1···O5$^{v}$ | 0.93(3) | 1.98(6) | 2.81(2) | 148(8) |
| O2W—H2W2···O2$^{i}$ | 0.94(3) | 2.01(7) | 2.80(2) | 141(8) |
| O2W—H1W2···O2 | 0.95(3) | 1.90(5) | 2.77(2) | 152(8) |
| O1W—H2W1···O5 | 0.94(3) | 1.91(5) | 2.79(2) | 156(9) |
| O1—H1···O1W$^{vi}$ | 0.95(3) | 1.71(5) | 2.61(2) | 157(8) |
| O4—H4···O2W$^{vii}$ | 0.95(3) | 1.83(6) | 2.67(2) | 146(8) |

Symmetry code(s): (i) $x-1, y, z$; (ii) $-x+1, -y+2, -z+1$; (iii) $-x+1, -y+1, -z+1$; (iv) $-x+2, -y+1, -z+1$; (v) $x+1, y, z$; (vi) $x, y-1, z$; (vii) $x, y+1, z$.

tural model leads to more precise results as reflected from the geometrical parameters and the agreement factors ($R(F^2) = 0.018$ and $wR(F^2) = 0.043$ for the $P\bar{1}$ model compared to the values of 0.025 and 0.061 respectively for the $P1$ model). As discussed above, such subtle structural changes might explain the unusual thermal behavior of unit cell parameters between 140 K and 100 K (see Fig. 3). On the other hand, the FT-IR measurements, discussed hereafter, show significant changes on cooling and heating the sample below 130 K. Thereafter, we compare the two structural models: $P1$ at 225 K and $P\bar{1}$ at 100 K. The crystal structures show no obvious changes at the two different temperatures. The two symmetry-independent molecules have very similar geometrical parameters (Table 2). At 100 K, the anionic moieties are characterized by distorted tetrahedral geometry around the selenium atom, where each central selenium atom is connected to two terminal oxygen atoms (Se1—O3: 1.6654(8) Å and Se1—O2: 1.6789(9) Å) with significantly shorter bond lengths than the protonated Se1—OH bond (Se1—O1: 1.7735(8) Å). At 225 K, the two inorganic anions still adopt the distorted configuration. Inside the $(HSeO_3)^-$ tetrahedra the Se—O bond lengths range from 1.646(14) Å to 1.682(14) Å and are shorter by ~0.105(14) Å than the Se—OH bonds (Se1—O1: 1.752(14) Å and Se1—O1: 1.790(11) Å). One can notice that the Se—O bond lengths are different at both temperatures. These differences are well correlated with the number and the strength of the hydrogen bonds formed by the oxygen atoms. The terminal oxygen atoms O2 (at 100 K) and O2 and O5 (at 225 K) are involved in three hydrogen bonds: one O—H···O and two N—H···O (see Table 3) whereas, O3 (at 100 K) and O3 and O6 (at 225 K) are involved in only two N—H···O hydrogen bonds.

Similar to other anilinium compounds [25,28,36], the organic cations exhibit the characteristic distortion features of the aromatic ring from the ideal hexagonal form. At both temperatures, the organic cations still disordered over two orientations as also observed at room temperature (Fig. 5). At 225 K the two independent aromatic rings are rotated around the C1—C4 and C7—C10 molecular axes by 53.50(4)° and 54.97(3)° respectively. By decreasing the temperature to 100 K the organic cation is less disordered and the rotation angle of the aromatic ring changes to 54.73(2)°. Interestingly, the deviation of the nitrogen atoms from the mean plane of the aromatic rings is different at both temperatures. At 100 K, the N1 atom is displaced by 0.030(2) Å and 0.041 (2) Å from the mean planes formed by the two parts of the disordered cation. At 225 K, the displacement of the N1 and N2 atoms range from 0.010(3) Å to 0.063 Å. These deviations are associated with the out-of-plane bending of the ammonium group and indicate that the deformation of the ammonium group is affected by the temperature changes.

The hydrogen-bond network was basically preserved (Table 3). Indeed, no significant changes in the crystal packing occurred on cooling the sample from 225 to 100 K. The main differences are related to changes in the number of N—H···O and O—H···O hydrogen bonds as a result of breaking symmetry induced by the phase transition. Thus, two non-equivalent hydrogen bonds at 225 K are

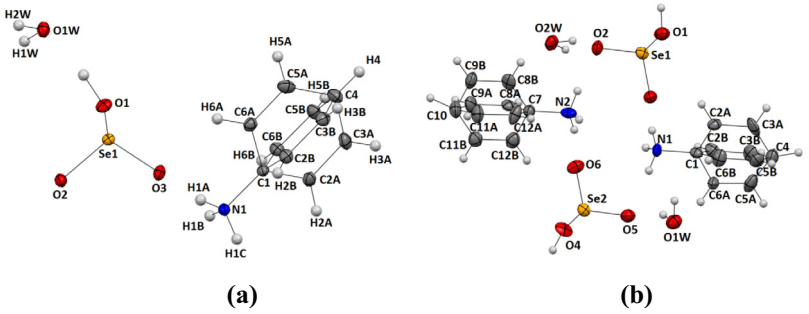


**Fig. 5.** The asymmetric unit of $[(C_6H_8N)^+, (HSeO_3)^-, H_2O]$ (a) at 100 K and (b) at 225 K, showing the atom-labeling scheme. Displacement ellipsoids are drawn at the 50% probability level and H atoms are shown as small gray spheres of arbitrary radii.

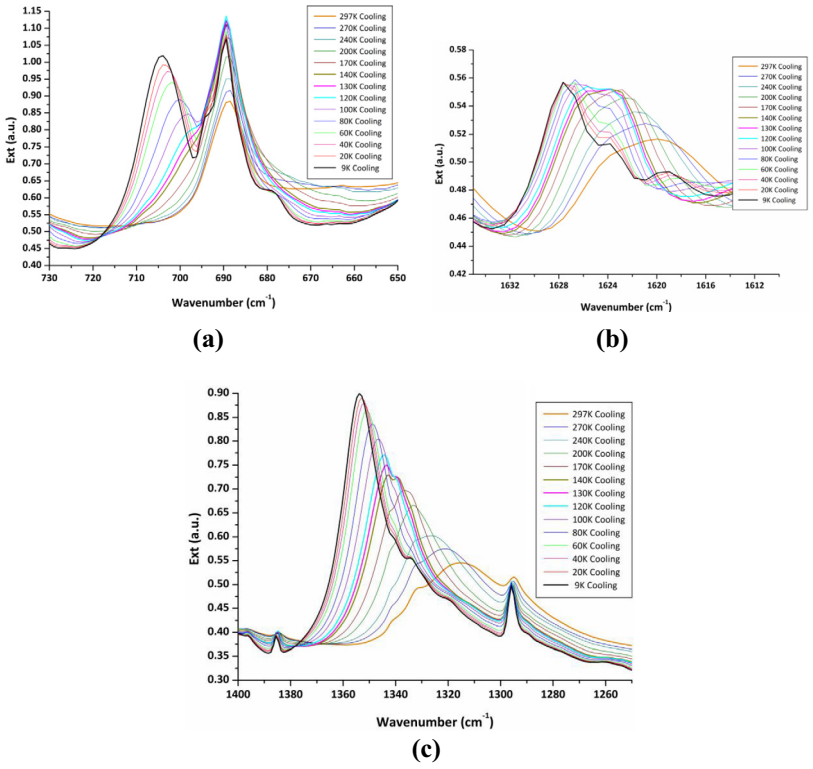


**Fig. 6.** The temperature-dependent (300–9 K) FT-IR spectra of $[(C_6H_8N)^+, (HSeO_3)^-, H_2O]$. (a) The spectral region corresponding to the $NH_3^+$ wagging mode. (b) The spectral region associated with the $NH_3^+$ scissoring mode. (c) The region of stretching C—N vibrations.

substituted by two symmetrically equivalent hydrogen bonds at 100 K.

### 3.3. Complementary FT-IR investigation

The IR spectroscopy was used as a complementary tool for the variable-temperature structural analysis. The FT-IR measurements were performed in the spectral range of 400–4000 $cm^{-1}$ by cooling and heating the sample (KBr pellets) in the temperature range of 300–9 K (see Fig. 1s; Supporting information). The assignment of the observed bands was essentially based on the reported studies concerning the vibrational spectra of the anilinium compounds [23,37,38]. Only the most important changes (induced by the variation of the temperature) are discussed in this part. The temperature evolution of the chosen regions of FT-IR spectra are presented in Fig. 6. As the temperature decreases from room temperature down to 9 K, significant changes arise below 140 K. The first dominant spectral changes are observed in the region of the $NH_3^+$ wagging mode. As can be seen in Fig. 6a, the intensity of the band located at 690 $cm^{-1}$ increases by decreasing the temperature and starts to split into two bands below 140 K. The intensity of the new band located at 705 $cm^{-1}$ increases by decreasing the temperature and has almost the same intensity as the original band located at 690 $cm^{-1}$ at 9 K. The second noticed changes are observed in the 1610–1632 $cm^{-1}$ spectral region associated with the $NH_3^+$ scissoring mode (Fig. 6b). The same trend as for the $NH_3^+$ wagging mode is observed. The broad structured band with the center at 1620 $cm^{-1}$ (at room temperature), splits into two bands at 1624 and 1628 $cm^{-1}$ with decreasing temperature. Finally, significant spectral changes are detected in the region 1260–1400 $cm^{-1}$ assigned to the stretching modes of the C—N groups. The intensity of the broad structured band with the center at 1315 $cm^{-1}$ increases with decreasing the temperature and splits to two bands with maxima at 1338 and 1342 $cm^{-1}$ below 140 K. It is notable that the observed spectral changes are reversible upon heating the sample from 9 K up to 300 K (see Fig. 2s, Supporting information). These results suggest the existence of a subtle structural reorganisation around 140 K and is consistent with the results of the structural analysis which showed that the deformation of the ammonium group is affected by the temperature changes. The observed spectral changes essentially associated with the vibrations of the ammonium group ($NH_3^+$) could be explained by the subtle rearrangement of hydrogen atoms. We also investigated the spectral region (above 3000 $cm^{-1}$) corresponding to the intermolecular interactions network (see Fig. 3s, Supporting information). Unfortunately, all the modes for O—H...O and N—H...O hydrogen bonds in the spectra overlap and form broad bands even at low temperatures. This could be explained by the similar donor–acceptor distances in the hydrogen bonding network. Additionally, it is well known that this spectral region contains also the contributions of the stretching vibrations of water molecules and ammonium groups as well as the aromatic C—H stretching vibrations. Therefore, it was not possible to extract the appropriate bands of the different hydrogen bonds and to correlate them to the temperature induced changes.

## 4. Conclusion

The present study reports the structural characterization, the differential scanning calorimetry analysis and the FT-IR spectroscopic investigations of a new anilinium–selenious hybrid compound. The crystal packing consists of alternating layers of anilinium cations and hydrogenselenite anions interconnected by N—H...O hydrogen bonds. The water molecules are located within the anionic layers and are involved in the strongest O—H...O intermolecular interactions connecting the hydrogenselenite anions. The organic cations are disordered over two orientations even at

low temperature. The temperature dependent changes of the unit cell parameters exhibit an anomalous behavior at temperatures between 140 and 110 K. We have shown that such unexpected behavior could be explained by the subtle non-centrosymmetric to centrosymmetric structural phase transition that occurs on cooling the crystal from 225 K to 100 K. The accurate structural analysis at 225 K and at 100 K reveals that the deformation of the ammonium group is affected by the temperature changes. The infrared measurements show significant changes on cooling and heating the sample around 140 K. The observed spectral changes essentially associated with the vibrations of the ammonium group ($NH_3^+$) are consistent with the results of the structural analysis. Both the structural and the infrared results indicate that the molecular rotation of the aromatic rings around the C1—C4 (and C7—C10 at 225 K) affect the vibrational modes of the ammonium group and could be the origin of the subtle structural phase transition.

## Acknowledgements

This work was supported by the Université de Lorraine, the CNRS and the Institut Jean Barriol, which are gratefully acknowledged. R.T. is indebted to the Algerian Ministry of Research and Université Abbes Laghrour-Khenchela for a doctoral fellowship.

## Appendix A. Supplementary material

CCDC 1425772–1425774 contains the supplementary crystallographic data for this paper. These data can be obtained free of charge from The Cambridge Crystallographic Data Centre via www.ccdc.cam.ac.uk/data_request/cif. Supplementary data associated with this article can be found, in the online version, at http://dx.doi.org/10.1016/j.ica.2016.02.047.

## References

[1] M. Mas-Torrent, S.S. Turner, K. Wurst, J. Vidal-Gancedo, X. Ribas, J. Veciana, P. Day, C. Rovira, Inorg. Chem. 42 (2003) 7544.
[2] F. Setifi, S. Golhen, L. Ouahab, A. Miyazaki, K. Okabe, T. Enoki, T. Toita, J.I. Yamada, Inorg. Chem. 41 (2002) 3786.
[3] M.R. Bryce, M.C. Petty, Nature (London) 374 (1995) 771.
[4] J. Peng, E.B. Wang, Y.S. Zhou, Y. Xing, Y.H. Lin, H.Q. Jia, Y.J. Shen, J. Chem. Soc., Dalton Trans. (1998) 3865.
[5] G. Rombaut, S.S. Turner, J. Chem. Soc., Dalton Trans. (2001) 3244.
[6] J.L. Bredas, C. Adant, P. Tackx, A. Persoons, Chem. Rev. 94 (1994) 243.
[7] A.-Y. Li, S.-W. Wang, J. Mol. Struct. 807 (2007) 191.
[8] B.-H. Peng, G.-F. Liu, L. Liu, D.-Z. Jia, Tetrahedron 61 (2005) 5926.
[9] E. Yang, X.-Q. Wang, Y.-Y. Qin, Chin. J. Struct. Chem. 11 (2006) 1365.
[10] W.-B. Yang, C.-Z. Lu, H.-H. Zhuang, Chin. J. Struct. Chem. 2 (2002) 168.
[11] R.-B. Fu, X.-T. Wu, S.-M. Hu, W.-X. Du, Chin. J. Struct. Chem. 8 (2004) 855.
[12] Z.-H. Hu, Z.-L. Huang, D.-C. Zhang, Chin. J. Struct. Chem. 4 (2004) 376.
[13] H.-P. Zhou, Y.-M. Zhu, J.-J. Chen, Z.-J. Hu, J.-Y. Wu, Y. Xie, M.-H. Jiang, X.-T. Tao, Y.-P. Tian, Inorg. Chem. Commun. 9 (2006) 90.
[14] J. Whsyner, L. Verga, G.M. Williams, Pharmacol. Ther. 71 (1996) 107.
[15] P. Hohenberg, W. Kohn, Phys. Rev. B 136 (1964) 864.
[16] A. Altun, K. Golcuk, M. Kumru, J. Mol. Struct. (THEOCHEM.) 17 (2003) 625.
[17] J. Hartmann, A. Weiss, Z. Naturforsch. Teil. A 46 (1991) 367.
[18] V.G. Krishnan, A. Weiss, Ber. Bunsenges. Phys. Chim. 87 (1993) 254.
[19] K. Bouchouit, Z. Sofiani, B. Derkowska, S. Abed, N. Benali-cherif, M. Bakasse, B. Sahraoui, Opt. Commun. 278 (2007) 180.
[20] G.J. Perpétue, J. Janczak, Acta Crystallogr. C60 (2004) 768.
[21] S. Shigeto, H. Hiramatsu, H.-O.J. Hamaguchi, Phys. Chem. A110 (2006) 3738.
[22] K. Bouchouit, H. Bougharraf, B. Derkowska-Zielinska, N. Benali-cherif, B. Sahraoui, Opt. Mater. 48 (2015) 215.
[23] I. Matulková, J. Cihelka, K. Fejfarová, M. Dušek, M. Pojarová, P. Vaněk, J. Kroupa, M. Šála, R. Krupková, I. Němec, CrystEngComm 13 (2011) 4131.
[24] A. Cabana, C. Sandorfy, Can. J. Chem. 40 (1963) 622.
[25] E.-E. Bendeif, S. Dahaoui, M. François, N. Benali-Cherif, C. Lecomte, Acta Crystallogr. B61 (2005) 700.
[26] N. Benali-Cherif, A. Direm, F. Allouche, L. Boukli-H-Benmenni, S. Soudani, Acta Crystallogr. E63 (2007) 2054.
[27] N. Benali-Cherif, A. Direm, F. Allouche, S. Soudani, Acta Crystallogr. E63 (2007) 2272.
[28] Z. Boutobba, A. Direm, N. Benali-Cherif, Acta Crystallogr. E66 (2010) o595.
[29] N. Benali-Cherif, F. Allouche, A. Direm, L. Boukli-H-Benmenni, K. Soudani, Acta Crystallogr. E63 (2007) 2643.
[30] N. Dadda, A. Nassour, B. Guillot, N. Benali-Cherif, C. Jelsch, Acta Crystallogr. A68 (2012) 452.
[31] F.H. Allen, Acta Crystallogr. B58 (2002) 380.
[32] Oxford Diffraction, CrysAlis CCD and CrysAlis RED (Versions 1.171.33.48), Oxford Diffraction Ltd, Abingdon, Oxfordshire, England, 2009.
[33] G.M. Sheldrick, Acta Crystallogr. A64 (2008) 112.
[34] L.J. Farrugia, J. Appl. Crystallogr. 32 (1999) 837.
[35] R. Takouachet, R. Benali-Cherif, N. Benali-Cherif, Acta Crystallogr. E70 (2014) o186.
[36] J.A. Paixaõ, A. Matos Beja, M. Ramos Silva, J. Martin-Gil, Acta Crystallogr. C56 (2000) 1132.
[37] M.K. Marchewka, J. Janczak, S. Debrus, J. Baran, H. Ratajczak, Solid State Sci. 5 (2003) 643.
[38] J. Cihelka, D. Havlicek, R. Gyepes, I. Němec, Z. Koleva, J. Mol. Struct. 980 (2010) 31.